A-M/AGC WEIGHTED PRE-DETECTION DIVERSITY COMBINING

E. R. Hill

Summary. A method has been proposed[1,2] for improving the performance of automatic gain control (agc) weighted diversity combiners in the presence of fast fading radio-frequency (rf) signals by use of the amplitude modulation (a-m)(detected linear intermediate-frequency (i-f) envelope) in addition to the agc voltage to weight the combiner. Also suggested[1] was a method for selecting the channel with the best signal-to-noise ratio (SNR) by use of the a-m and agc voltages. Experimental hardware has been constructed for evaluation of three configurations: an a-m/agc weighted combiner; an a-m/agc based selector; and an a-m/agc combiner/selector where the criterion for combine or select is determined by the phase error between the two channels. An experimental study was also conducted[3] of the phase-locked loop (PLL) to determine the best configuration and parameter values for the combiner application (where relatively large phase errors are permissible). Data were taken under laboratory and operational (Vandenberg Air Force Base) conditions and are compared with data taken with a commercial agc weighted combiner.

Introduction. Radio waves in the earth's environment can experience variations in signal level (fading) due to absorption, refraction, reflection etc. When more than one signal can be obtained from the same source with uncorrelate, fading characteristics, these are called diversity signals. These may be obtained for example, from different antennas, from different polarizations, from the same antenna or by use of more than one frequency. The object of diversity combining is, by use of two or more diversity signals, to obtain a single signal which is better, on the average, than any one signal or at least as good as the better signal. Conventional pre-detection diversity combiners use only the receiver agc voltages to weight the i-f signals before linearly adding them. Such combiners are optimum (i.e., maximize the output SNR) only if the agc systems can track the fades in the rf signal levels (i.e., to maintain the linear i-f signals at constant amplitude). This limitation can be overcome by using the a-m (linear i-f envelope) voltages in addition to the agc voltages to weight the combiner.[1]

Mr. Hill is with the Instrumentation Department of the Pacific Missile Test Center, Point Mugu, CA.

This work was sponsored by the Naval Air Systems Command under a task assignment in support of the Telemetry Group of the Range Commanders Council.

One of the prime motivations for this work is the serious loss of data from flame attenuation during the launch of multi-stage missiles (Vandenberg AFB).[4]

The purpose of this paper is to present performance data on the three basic configurations described in the summary and to compare this data with that of the agc weighted combiner. Block diagrams are presented and the fundamental theory given. Schematics and details of implementation are available in a Pacific Missile Test Center technical report to be published. Most of the mathematical background and theory appears in reference 1 and due to space limitations cannot be repeated here.

Review of Diversity Combining Theory. A review of the theoretical basis of agc weighted combiners will first be presented. Also, the theoretical justification for the three experimental configurations will be given in addition to block diagrams for their implementation. It has been proven[5] that the optimum weighting coefficient for a linear diversity combiner is equal to the ratio of the rms signal voltage to the mean square noise voltage. In terms of the dual channel combiner configuration in Figure 1, the optimum combining ratio a_R is given by

$$a_R = \frac{\frac{S_1}{N_1^2}}{\frac{S_2}{N_2^2}} = \left(\frac{S_1}{S_2}\right)\left(\frac{N_2^2}{N_1^2}\right) \tag{1}$$

where S_1 and S_2 are the rms signal voltages, and N_1^2 and N_2^2 are the mean square noise voltages of channels one and two respectively. An rf receiver and its agc system (actually internal to the receiver) can be modeled as in Figure 2 where

$e_s(t)$ = rf input signal voltage

e_g = agc voltage

e_a = the average absolute value of the output signal voltage S (t)

The combining ratio of an agc weighted combiner is derived on the assumption that the receiver agc systems are able to track any variations in the rf signal levels so as to maintain the output rms signal voltages S_1 and S_2 constant (and thus equal). Under this assumption, equation (1) reduces to

$$a_R = \frac{N_2^2}{N_1^2} \tag{2}$$

or as the ratio of the signal-to-noise power ratios

$$a_R = \frac{\left(\frac{S_1}{N_1}\right)^2}{\left(\frac{S_2}{N_2}\right)^2} \tag{3}$$

as it is often expressed. The rnean square noise at the output of the receiver can be expressed[1] as a function of the agc voltage as follows:

$$N^2 = \left(\frac{\pi}{2\sqrt{2}}\right)^2 \left(K_2 \; V \; n_e\right)^2 \; 10^{\frac{2e_g}{K_1}} \tag{4}$$

where V = the bias voltage of the agc integrator

$\frac{\pi}{2\sqrt{2}}$ = ratio between rms and average absolute value of a sinusoid. The constants K_1 and K_2 come from the equation which relates the agc voltage to the static rf signal strength e_s (expressed in volts rms) $e_g = - K_1 \log K_2 \, e_s$

and (5)

$$n_e = \sqrt{kTBRF} \tag{6}$$

where

- n_e = receiver effective input rms noise voltage
- k = Boltzmann's constant
- T = absolute temperature (degrees Kelvin)
- B = effective receiver bandwidth
- R = receiver input impedance
- F = receiver noise figure

By substituting equation (4) (expressed for each receiver) into equation (2) the optimum combing ratio for an agc weighted combiner is obtained

$$a_R = 10^{\frac{2}{K_1}\left(e_{g2} - e_{g1}\right)} \tag{7}$$

When the fades in the rf signal level occur at a rate which the agc system cannot track, the agc weighted combiner is no longer optimum and the i-f output amplitudes in equation (1) must be considered. For implementation purposes, the average absolute value e_a (full-wave rectified average) can be obtained with less error, in the presence of noise, than the rms and, since the two differ on by a constant, equation (1) becomes (with the aid of equations (2) and (7)

$$a_R = \left(\frac{e_{a1}}{e_{a2}}\right) 10^{\frac{2}{K_1}\left(e_{g2} - e_{g1}\right)} \tag{8}$$

The average absolute value of S (t) is approximated by taking the average absolute value of signal plus noise with the circuit shown on Figure 3. The output of this circuit is the expectation of the absolute value of signal plus noise.[6]

$$e_o = E\left\{\left|S(t)+N(t)\right|\right\} = \frac{A}{\sqrt{2\pi x}}\left[(1 + 2x)\ I_o(x) + 2xI_1(x)\right] e^{-x} \tag{9}$$

where x is equal to half the signal-to-noise power ratio, A is the peak amplitude of the sinusoidal carrier, $I_o(x)$ and $I_1(x)$ are the modified Bessel functions of the first kind.

The theoretical and experimental values as a function of i-f SNR appear in Figure 3 where the output has been normalized by dividing by e_a (the average absolute value of the sinusoidal signal component). To place equation (8) in a form more easily implemented, use the following identity

$$\left(\frac{e_{a1}}{e_{a2}}\right) = 10^{\frac{2}{K_1}\left[\left(\frac{K_1}{2}\right)\log\left(\frac{e_{a1}}{V}\right) - \left(\frac{K_1}{2}\right)\log\left(\frac{e_{a2}}{V}\right)\right]} \tag{10}$$

and rewrite equation (8) as

$$a_R = 10^{(e_{w2} - e_{w1})} \tag{11}$$

where the weighting signals e_{w1} and e_{w2} are equal to

$$e_{w1} = \frac{2}{K_1}\ e_{g1} - \log\left(\frac{e_{a1}}{V}\right) \tag{12}$$

and

$$e_{w2} = \frac{2}{K_1}\ e_{g2} - \log\left(\frac{e_{a2}}{V}\right) \tag{13}$$

A block diagram implementation of these weighting signals for use with a commercial agc weighted combiner appears in Figure 4. The first of the three experimental combiners, the a-m/agc weighted combiner, appears in Figure 5 and is similar to the commercial combiner configuration except for the PLL parameters which will be discussed in the next section.

It was suggested[1] that an optimum diversity selector could be constructed by use of the following equation:

$$e_s = \left(\frac{1}{K_2\ V}\right)\left(\frac{e_a}{10^{\frac{e_g}{K_1}}}\right) \tag{14}$$

to determine the receiver channel with the greater rf input signal level and thus the greater output SNR.

Equation (14) shows that the rf input signal level can be determined from the linear i-f envelope and the agc voltage. To place equation (14) in a form more easily implemented, rearrange and take the logarithm (base ten) of each side.

$$\log\left(K_2 e_s\right) = \log\left(\frac{e_a}{V}\right) - \frac{e_g}{K_1} \tag{15}$$

When equation (15) is expressed for each receiver channel and the second equation subtracted from the first, the following equation is obtained:

$$e_L = \log\left(\frac{e_{s1}}{e_{s2}}\right) = -\frac{e_{g1}}{K_1} + \log\left(\frac{e_{a1}}{V}\right) + \frac{e_{g2}}{K_1} - \log\left(\frac{e_{a2}}{V}\right) \tag{16}$$

Equation (16) describes an implementation by which a signal voltage can be obtained which is equal to the logarithm of the ratio of the rf input signal levels. The signal voltage e_L is well suited as a selector signal since it will be zero when the rf signal levels are equal, positive when channel one is greater than channel two, and negative when channel two is greater than channel one. In addition, it provides logarithmic compression of the dynamic range. Since the i-f SNR and rf signal level are related[1] by

$$\frac{S}{N} = \frac{e_s}{n_e} \tag{17}$$

equation (16) can be expressed in terms of the ratio of the linear i-f signal-to-noise ratios

$$e_L = \log \frac{\left(\frac{S_1}{N_1}\right)}{\left(\frac{S_2}{N_2}\right)} \tag{18}$$

Equation (16) can be implemented by the differential operational amplifier weighting and summing circuit in Figure 6. The second experimental combiner configuration, the optimum a-m/agc based selector, appears in Figure 7. The comparator thresholds were set for ± 6 dB for the data to be presented.

The third experimental model, the a-m/agc combiner/selector, was designed with the objective of overcoming some of the shortcomings of the first two. First, it was observed that a large proportion of the errors which occured as a result of high frequency fading in the presence of noise resulted from the inability of the phase-locked loop to maintain an acceptablly small phase error between the two carrier signals. A sufficiently large phase error causes degradation rather than enhancement of the output signal. Second, it was

observed that an optimum selector produces additional errors in the process of switching between the two carrier signals. This arises from the fact that the two carriers are not necessarily phase aligned at the time of switching. Thus a step in phase occurs in the output signal at the time of switching which produces an impulse at the output of an fm demodulator or a step at the output of a pm demodulator. These facts lead to the conclusion that combining should continue to the point where the phase error causes the combined output SNR to become less than the SNR of the better single channel, at which time that better channel should be selected. With reference to Figure 1, use of the Law of Cosines, and the usual assumptions[5] of uncorrelated noise sources etc., the output SNR can be written as a function of the phase angle θ between the two carrier components

$$\frac{S_o}{N_o} = \frac{\sqrt{(a_R S_1)^2 + S_2^2 + 2 a_R S_1 S_2 \cos\theta}}{\sqrt{(a_R N_1)^2 + N_2^2}} \tag{19}$$

By substituting equation (1) into equation (19), The output SNR of an optimum combiner becomes

$$\frac{S_o}{N_o} = \frac{\sqrt{\left(\frac{S_1}{N_1}\right)^4 + \left(\frac{S_2}{N_2}\right)^4 + 2\left(\frac{S_1}{N_1}\right)^2\left(\frac{S_2}{N_2}\right)^2 \cos\theta}}{\sqrt{\left(\frac{S_1}{N_1}\right)^2 + \left(\frac{S_2}{N_2}\right)^2}} \tag{20}$$

which is a function of the single channel SNRs and the phase angle between the carrier components. The critical phase angle θ_c can be obtained by solving for θ as a function of the input SNRs when the output SNR is equal to the SNR of the better single channel. Thus, assume

$$\frac{S_o}{N_o} = \frac{S_1}{N_1} \geqslant \frac{S_2}{N_2} \tag{21}$$

and solve for θ in equation (20)

$$\theta_c = \cos^{-1}\left[\frac{\left(\frac{S_1}{N_1}\right)^2 - \left(\frac{S_2}{N_2}\right)^2}{2\left(\frac{S_1}{N_1}\right)^2}\right] = \cos^{-1}\left[1 - \frac{\left(\frac{S_2}{N_2}\right)^2}{\left(\frac{S_1}{N_1}\right)^2}\right] \tag{22}$$

Examination of equation (2Z) indicates that when the single channel SNRs are equal, the critical phase angle is 90°, and when the number one channel SNR is much larger than the number two channel SNR, the critical phase angle approaches 60°; thus to summarize

$$1 \geq \frac{\left(\frac{S_2}{N_2}\right)^2}{\left(\frac{S_1}{N_1}\right)^2} \geq 0 \qquad 90^\circ \geq \theta_c \geq 60^\circ \tag{23}$$

From this we conclude that it never pays to combine if the phase angle between the two carriers exceed ± 90° and it always pays to combine if this phase angle is less than ± 60°. Although the critical phase angle θ_c could be monitored by proper use of the function expressed by equation (18), for a first try the third experimental configuration was implemented with fixed thresholds to select the channel with the greater SNR when θ exceeds ± 90° and to resume combining when θ is reduced to less than ± 60°. This 30° hysteresis also guards against switch chatter resulting from noise on the output of the 50 kHz low-pass filter (LPF) that monitors the phase detector output voltage. The block diagram of the a-m/agc weighted combiner/selector appears in Figure 8.

Phase-Locked Loop Study A study of the phase-locked loop (PLL) in the combiner application (large phase errors) was initiated when it was observed that the increased error rate in the presence of dynamic rf signals was caused more from phase errors than by non-optimurn weighting signals. Only the more important results of this study[3] will be given here. The basic PLL configuration evaluated is that appearing in Figures 5, 7, and 8. Three phase detectors were evaluated: the set-reset flip-flop (SR-FF), the exclusive-OR gate, and the multiplier. Both of the digital phase detectors were preceded at each input by low hysteresis (20 mv) Schmitt triggers and the multiplier inputs were preceded by limiters. The rf receiver input signals for this evaluation were produced by the simulator in Figure 9 with LPF-limited noise into the phase modulators. This simulator produces both phase and amplitude modulation of the output rf signals. The multiplier phase detector showed a small improvement over the digital phase detectors at low SNR due to its inherent bandwidth reduction with decreasing SNR. The damping factor proved a non-critical parameter and showed little influence from 0.5 to 0.9 (0.7 was used in the experimental implementations). The SR-FF phase detector was chosen for use in the experimental circuits since it has a wide frequency pull-in capability as well as a linear ± 180° phase detector range. The study[3] showed 10 kHz to be the maximum PLL bandwidth (-3 dB) without significant degradation of performance under static or low frequency dynamic conditions. This bandwidth was used in the experimental combiners.

Evaluation with Laboratory Simulators In the real world, a pre-detection diversity combiner must cope simultaneously with amplitude and phase variations of the carrier components. In the laboratory evaluation, tests were first devised to evaluate the performance of the different configurations to each of these variations independently. Then

pseudo real-world tests were devised to measure the performance where both amplitude and phase of the input signals were changing simultaneously.

In the data plots presented, the following abbreviated notation will be used. The evaluation data for the commercial combiner configuration in Figure 4 with either a-m or a-m/agc weighting will be identified by “COM. COMB. (AGC)” and “COM. COMB. (A-M/AGC)” respectively. The data for the experimental combiner in Figure 5 with either a-m/agc or agc weighting will be identified by “EXP. COMB. (A-M/AGC)” and “EXP. COMB. (AGC)” respectively. The data for the experimental a-m/agc based selector in Figure 7 will be identified by “EXP. SEL (A-M/AGC).” Data for the experimental a-m/agc weighted combiner/selector in Figure 8 will be indentified by “EXP. COMB. /SEL. (A-M/AGC).” The notations “CH1" and “CH2" indicate data for the uncombined channels one and two respectively.

The simulator in Figure 10 was devised to produce sinusoidal, out-of-phase fading with nominal phase modulation between the two output carriers. The two multipliers are driven with out-of-phase sinusoids adjusted for 20 dB fades and the attenuators are set for about 10 dB difference in the average output signal levels. For a combiner to maintain an optimum combining ratio for these signals, the weighting signal bandwidth must be greater than the sinusoidal modulation frequency. The data in Figure 11 is primarily a comparison of the commercial agc weighted combiner with the a-m/agc weighted experimental combiner. The receiver agc time constants were set for 0.1 ms for all tests and the effective weighting signal bandwidth of the experimental combiner was about 150 kHz. The bit error probability (BEP) is plotted in Figure 11 for fade rates from 200 Hz to 200 kHz. The method used to compare performance was to determine the change in SNR which would produce the observed change in BEP. The a-m/agc weighted experimental combiner parallels the channel having the smaller BEP with an average improvement of about 4 dB out to a fade rate of about 5 kHz after which it shows a steady increase in BEP to around 50 kHz, after which the increase is more rapid. Out to 200 kHz fade rate, the a-m/agc weighted experimental combiner is never less than 1 dB better than the better channel. The commercial agc weighted combiner at 200 Hz fade rate has nearly the same BEP as the experimental combiner, as would be expected, and parallels the better channel out to about 1 kHz fade rate where the BEP increases rapidly until it nearly equals the better channel at about 10 kHz. The agc weighted commercial combiner remains just below (about 0.1 dB) the better channel out to the maximum fade rate of 200 kHz. Also shown in Figure 11 is data taken with the experimental a-m/agc weighted combiner/ selector. Except for a couple of data point departures, the experimental combiner/selector shows the same performance as the experimental combiner out to about 20 kHz. However, from 50 kHz to 200 kHz, it shows a consistent improvement of about 0.3 dB. Presumably, large phase errors occur in this region which cause the combined output at times to have a lower SNR than the better channel.

The simulator in Figure 12 was devised to produce random phase modulation of the two RF signals, while at the same time maintaining constant and equal RF signal levels. The object being to test the combiner's ability to maintain phase coherency independent of its ability to maintain optimum weighting signals. In Figure 12, phase modulators are driven by independent gaussian noise sources whose bandwidths have been limited by low-pass filters. In Figure 13, the BEP is plotted with respect to these LPF bandwidths. The commercial a-m/agc weighted combiner in Figure 4 is compared with the a-m/agc weighted experimental combiner in Figure 5. The phase modulators produce about 60° rms phase modulation. The PLL bandwidth (-3 dB) of the experimental combiner was 10 kHz and that of the commercial combiner is believed to be about 2 kHz. The performance difference shown in Figure 13 is believed to be almost entirely due to this difference in PLL bandwidths. The experimental combiner BEP remains essentially constant out to a bandwidth of about 2 kHz and then increases to equality with the commercial combiner at about 20 kHz where neither combiner can cope with the high frequency and large amplitude phase modulation. The experimental combiner shows over 6 dB improvement in the region of 2 kHz phase modulation bandwidth. At 100 Hz there is less than 1 dB difference and they should become equal again at a sufficiently low bandwidth. It should also be noted in Figure 13 that the BEP for both the commercial and experimental combiner becomes worse than the better single channel BEP. This occurs for a phase modulation bandwidth of about 1.3 kHz for the commercial combiner and about 12 kHz for the experimental combiner. The random phase-modulated signals produced by the simulator in Figure 12 were the only test signals used which caused the combined output to be worse than the better single channel. The a-m/agc weighted combiner/selector was designed to guard against degradation of the combined signal, relative to the best single channel, due to large phase errors. Figure 14 shows data taken with this combiner under similar conditions to Figure 13 and the combiner /selector does show a 50% (0.7 dB) reduction in BEP in the 10 kHz to 20 kHz phase modulation bandwidth region. The experimental combiner and experimental combiner/selector show the same BEP in the 2 kHz to 3 kHz region as they should.

The final laboratory tests were run with pseudo real-world signals produced by the simulator in Figure 9 which simultaneously produces random amplitude and phase modulation of the output signals. The simulator was set to produce 20 dB fades in the output signals and the LPF bandwidths were varied from 100 Hz to 20 kHz. Figure 15 compares the commercial combiner with both agc and a-m/agc weighting with the experimental combiner also with both agc and a-m/agc weighting. The commercial and experimental combiners show essentially the same performance out to about 200 Hz where the BEP of the commercial combiner begins to rise as a result of its narrower PLL bandwidth. The wider PLL bandwidth of the experimental combiner keeps the BEP constant out to about 1 kHz before beginning to increase. The experimental combiner shows an average improvement of over 5 dB in the 1 kHz to 5 kHz bandwidth region as a

result of its wider PLL bandwidth. For both the commercial and experimental combiners, the BEPs for agc and a-m/agc weighting are essentially the same for modulation bandwidths out to about 2 kHz. However, from 2 kHz to 20 kHz, there is an average improvement in BEP of about 0.5 dB for the wider bandwidth a-m/agc weighting signal for both the experimental and commercial combiners. For the diversity signals produced by the simulator in Figure 9, the greater improvement in the bandwidth region from 200 Hz to 20 kHz results from the widening of the PLL bandwidth. However, the smaller improvement resulting from the wider bandwidth weighting signals will be sustained to higher frequencies as shown by the results in Figure 11.

The performance of the a-m/agc based experimental selector in Figure 7 is also plotted in Figure 15. The experimental selector selects the channel whose SNR is greater by 6 dB and will stay with that signal until the other channel becomes 6 dB better than the channel currently selected. The performance of the selector is about 1 dB worse than the experimental combiner out to 1 kHz modulation bandwidth where it begins to degrade just as the experimental combiner does. Although the selector is not dependent upon phase alignment for the same reason that the combiner is, its performance is also dependent upon phase alignment. As mentioned before, if the two carriers are out of phase at the same time of switching, a step in phase occurs in the output signal which results in an impulse at the output of an fm demodulator. In the frequency region between 10 kHz and 20 kHz, the performance of the experimental selector parallels that of the experimental combiner, however, with a degradation of about 0.4 dB. This performance is typical and the experimental selector was always found on the average to be inferior to either the experimental a-m/agc weighted combiner or the experimental a-m/agc weighted combiner/selector. Despite the poor performance of the experimental selector relative to the experimental combiner, it still performs better than the commercial combiner at fading bandwidths above 600 Hz. This is attributed entirely to the narrower PLL bandwidth of the commercial combiner.

Operational Tests The Space and Missile Test Center (SAMTEC) at Vandenberg Air Force Base, CA. has taken data on their missile launches with experimental combiner hardware supplied by the Pacific Missile Test Center PACMISTESTCEN at Point Mugu, CA. The first data were taken with an interface chassis (within dotted lines of Figure 4) which permitted the commercial combiner to be used with either its conventional agc weighting or with the a-m/agc weighting signals. Also included in the interface chassis was an experimental a-m/agc-based selector with output signals to operate into the commercial combiner weighting signal input points. This selector was thus dependent upon the narrower PLL bandwidth of the commercial combiner. A second series of operational tests[8] were conducted after the complete experimental combiner, selector, and combiner/selector shown in Figures 5, 7, and 8 were incorporated in the experimental chassis. SAMTEC found[7] that the commercial combiner with a-m/agc weighting provided

improvement in the recovery of data over the commercial combiner with agc weighting during periods of heavy multipath interference. SAMTEC also found[8] that the experimental a-m/agc weighted combiner and combiner/selector provided more error-free data than the agc weighted commercial combiner during third stage burn. In the laboratory evaluations, the a-m/agc weighted experimental combiner and combiner/selector were always found to be as good as or better than the agc weighted commercial combiner. This was not found to be true in the operational tests and some aspects of the results are not well understood at this time. The operational data was taken under such a wide range of conditions and circuit parameter values that no meaningful summary of data can be presented in the space available here. This data will be contained in a technical report to be published in the fall of 1977.

Conclusions

1. It has been demonstrated that the performance of agc weighted diversity combiners can be improved at high fade rates by proper use of the a-m (amplitude of the linear i-f signals) signals in addition to the receiver agc voltages.

2. Wider PLL bandwidths (relative to bandwidths incorporated in commercial combiners) result in improved combiner performance for high frequency phase perturbations, without significant degradation for low frequencies.

3. For a laboratory simulator which produced simultaneously random amplitude and phase perturbations of the two carrier signals, the greater combiner improvement resulted from widening the combiner PLL bandwidth than from widening the bandwidth of the combiner weighting signals. An even wider PLL bandwidth than the 10 kHz used might be practical. An adaptive PLL bandwidth might prove feasible lor the combiner application.

4. The optimum signal selector (selects channel with the better SNR) does not perform as well as the optimum combiner (both depending on the same PLL bandwidth).

5. An optimum combiner/selector (where selection is based on differential signal phase error) outperforms an optimum combiner for high frequency phase/amplitude perturbation without degradation for low frequency phase/ amplitude perturbation.

6. Since the experimental combiner/selector showed the best overall performance, it warrants further investigation. The phase angles at which the decision to combine or select is pre-set should be further examined with the possibility of adapting these angles to the ratio of the signal-to-noise ratios. Increasing the 50 kHz bandwidth of the LPF that monitors the phase angle would probably give additional improvement.

References

1. E. R. Hill, “Time Domain Analysis of an AGC Weighted Combiner,” Proc. International Telemetering Conference, Vol 9, pp. 475-494; October 1973.

2. E. R. Hill, “Time Domain Analysis of an Automatic Gain Control Weighted Diversity Combining System,” (Technical Publication TP-73-47) 14 December 1973, Naval Missile Center, Point Mugu, CA.

3. M. E. Novak, “An Investigation of Phase Lock Loop Requirements in Diversity Combiners”, Master thesis, California State University, Northridge, 1977.

4. R. G. Streich, D. E. Little, R. B. Pickett, “Dynamic Requirements for Diversity Combiners,” Proc. ITC, Vol 8, pp. 635-642; Ocober 1972.

5. D. G. Brennan, “Linear Diversity Combining Techniques,” Proc. IRE, June 1959.

6. J. B. Thomas, “An Introduction to Communication Theory,” John Wiley & Sons, Inc. New York, N. Y., p. 352, 1969.

7. “Diversity Combiner A-M/AGC Control Technique, “Report Number PA 100-76-48, Space and Missile Test Center, Vandenberg Air Force Base, California, 93437.

8. “A-M/AGC Combiner,” Report Number PA 100-76-68, Space and Missile Test Center, Vandenberg Air Force Base, California, 93437.

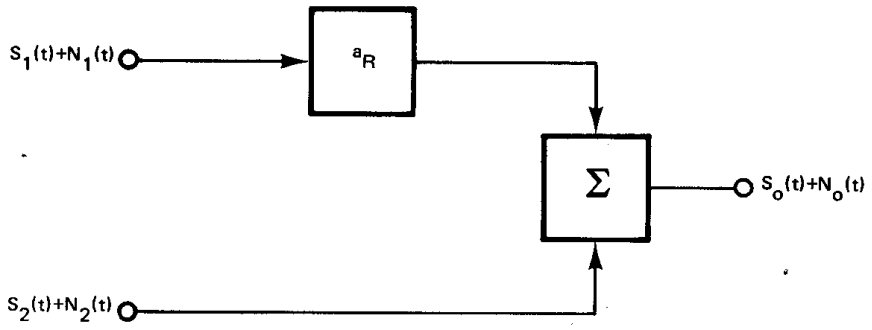

Figure 1. Diagram of Dual-Channel Linear Diversity Combiner.

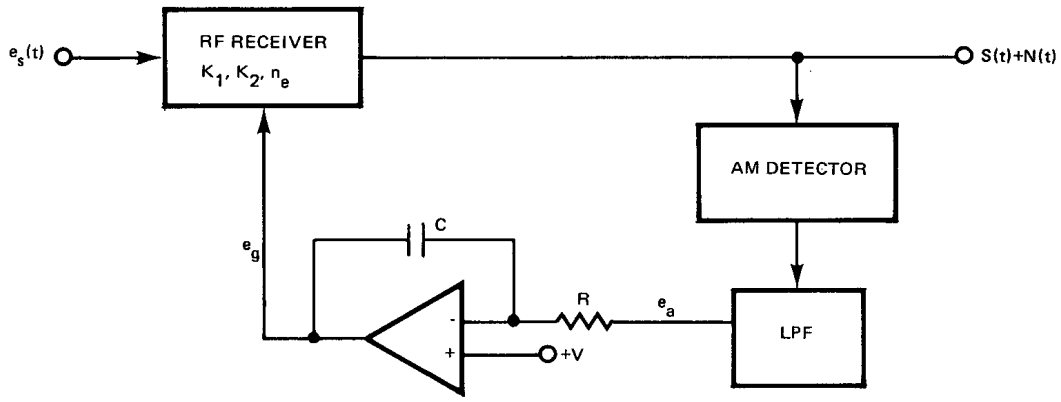

Figure 2. RF Receiver With AGC System.

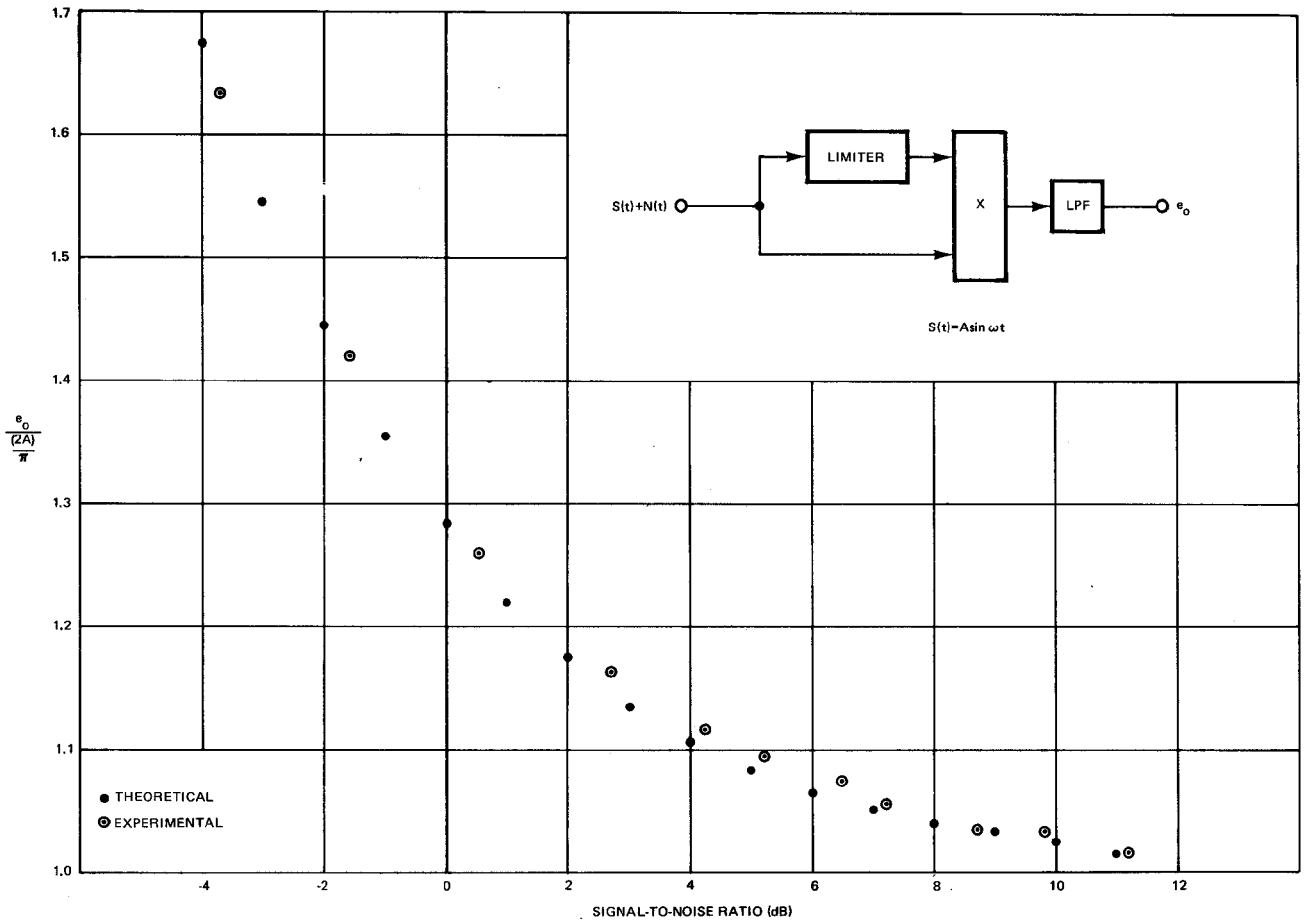

Figure 3. Theoretical and Experimental Data for the Average Absolute Value A-M Detector.

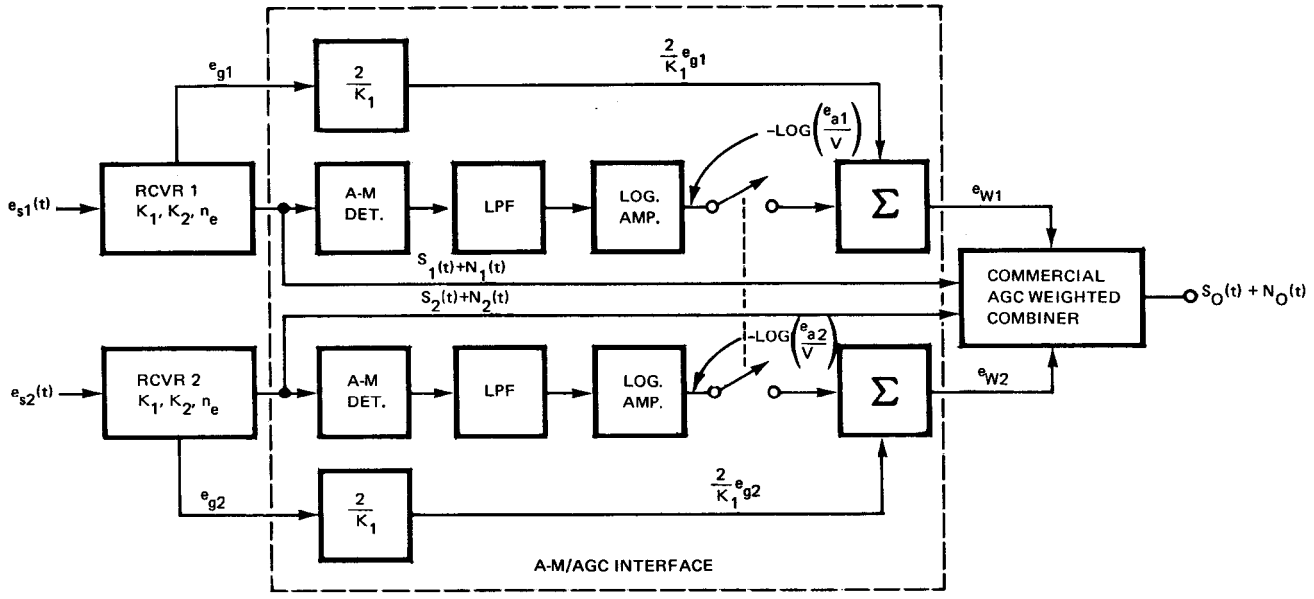

Figure 4. Commercial AGC Weighted Combiner With Option for A-M/AGC Weighting.

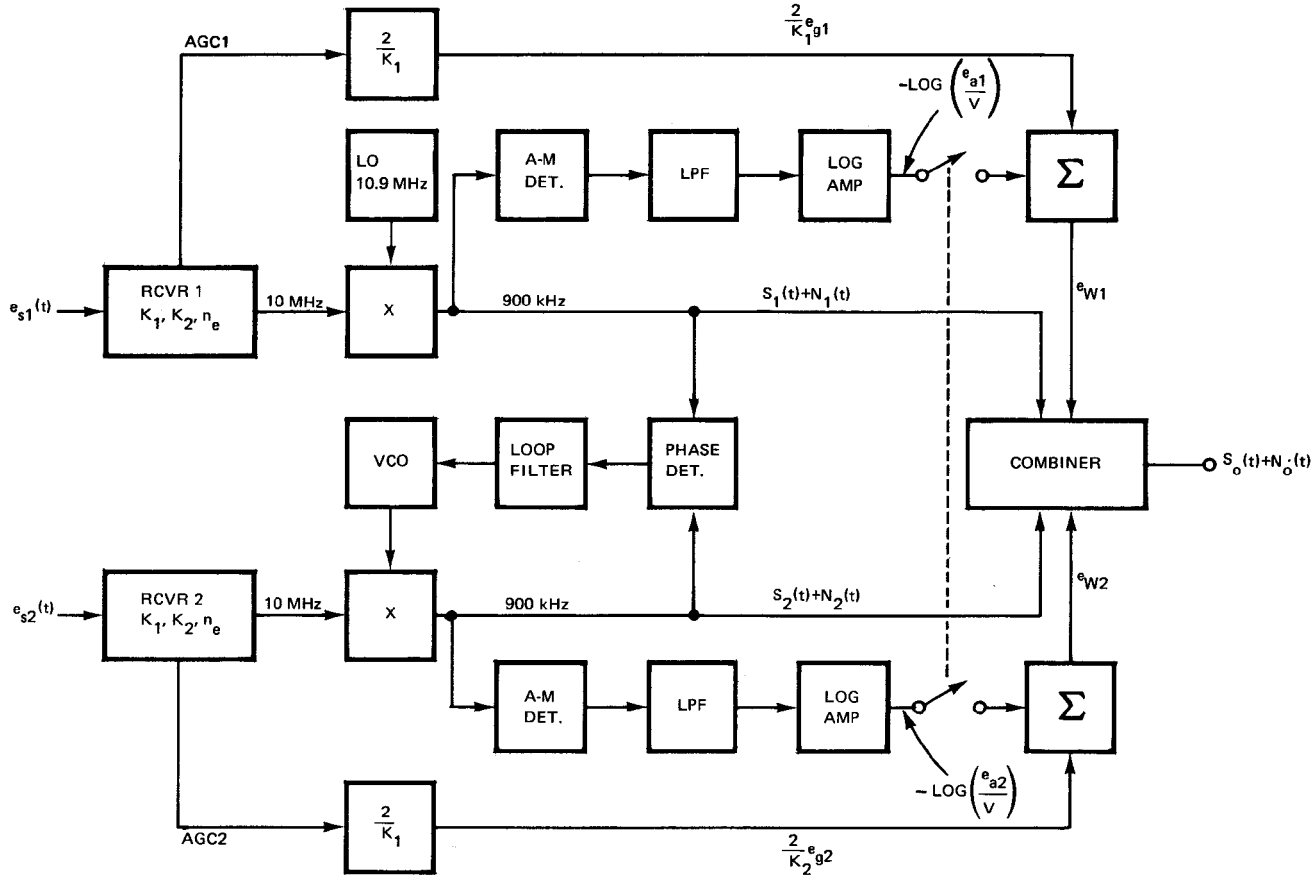

Figure 5. Experimental A-M/AGC Weighted Combiner With Option for AGC Weighting.

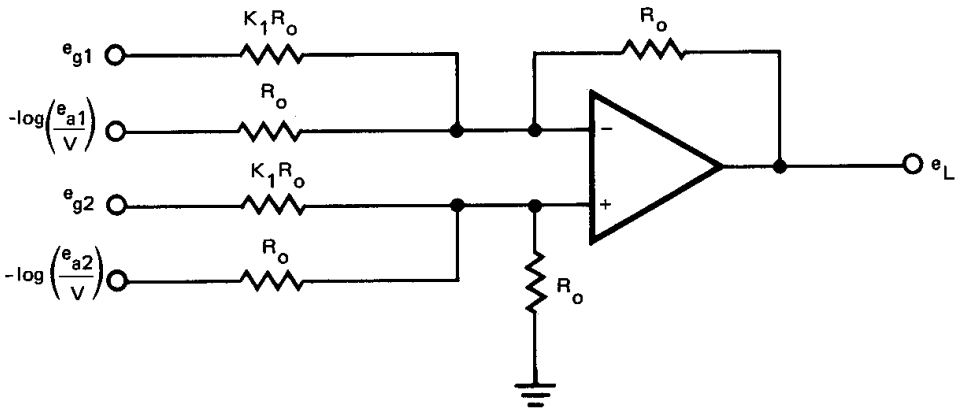

Figure 6. Differential Operational Amplifier Weighting and Summing Circuit.

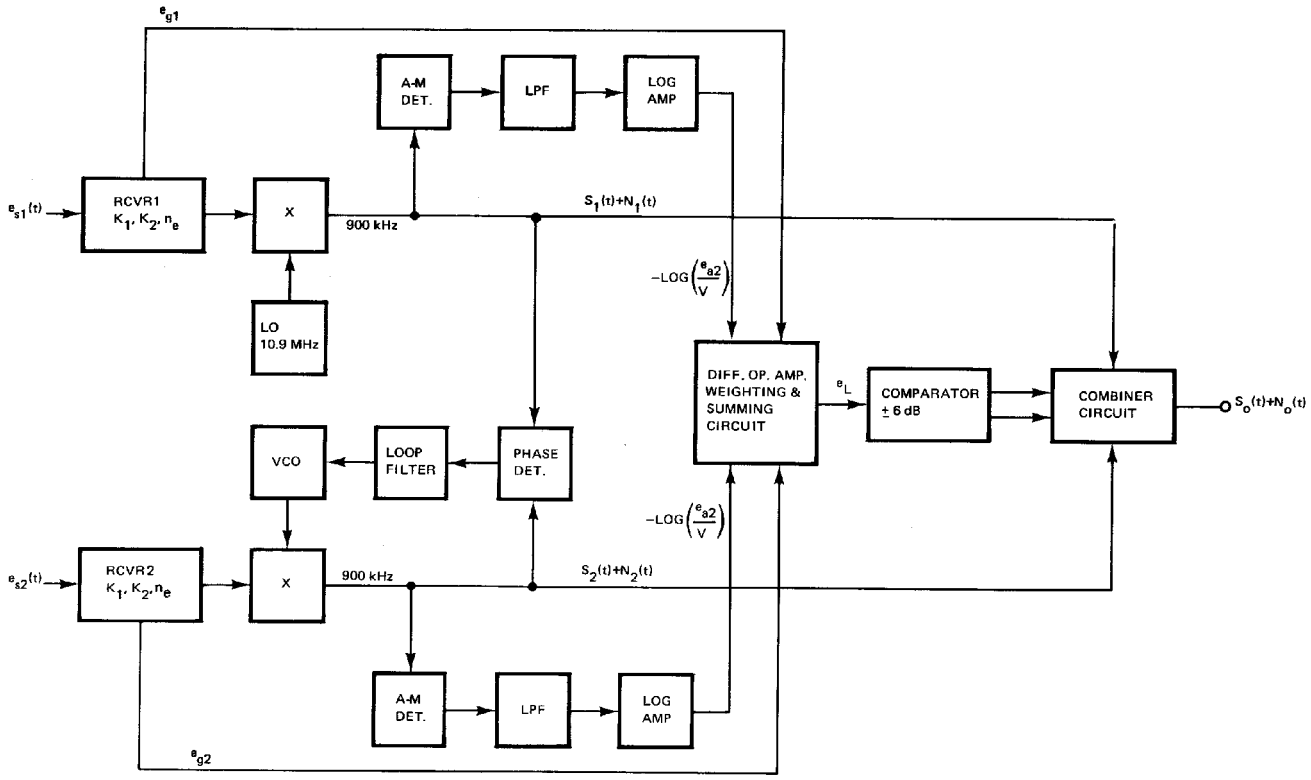

Figure 7. Experimental A-M/AGC Based Selector.

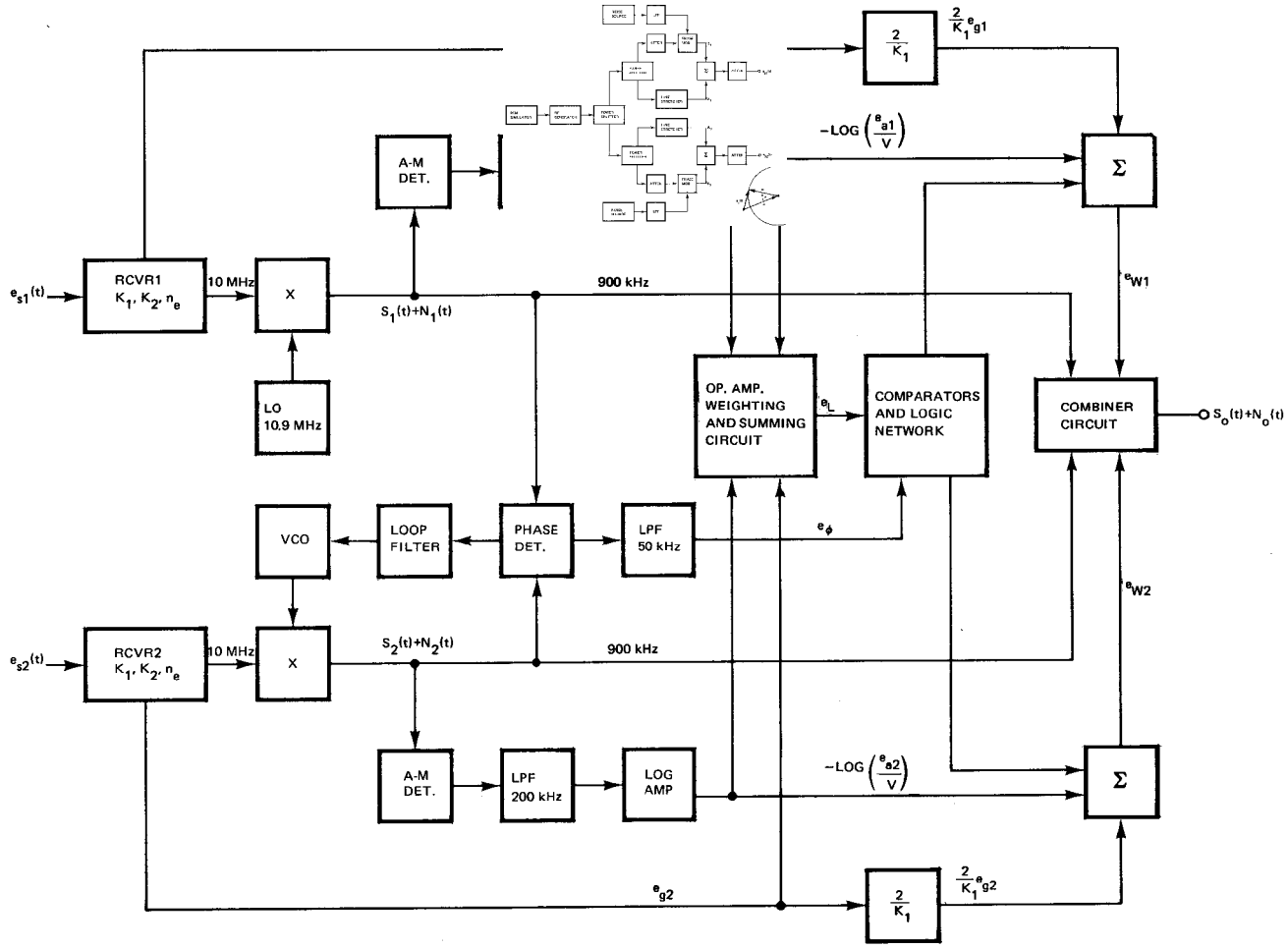

Figure 8. Experimental A-M/AGC Weighted Combiner/Selector.

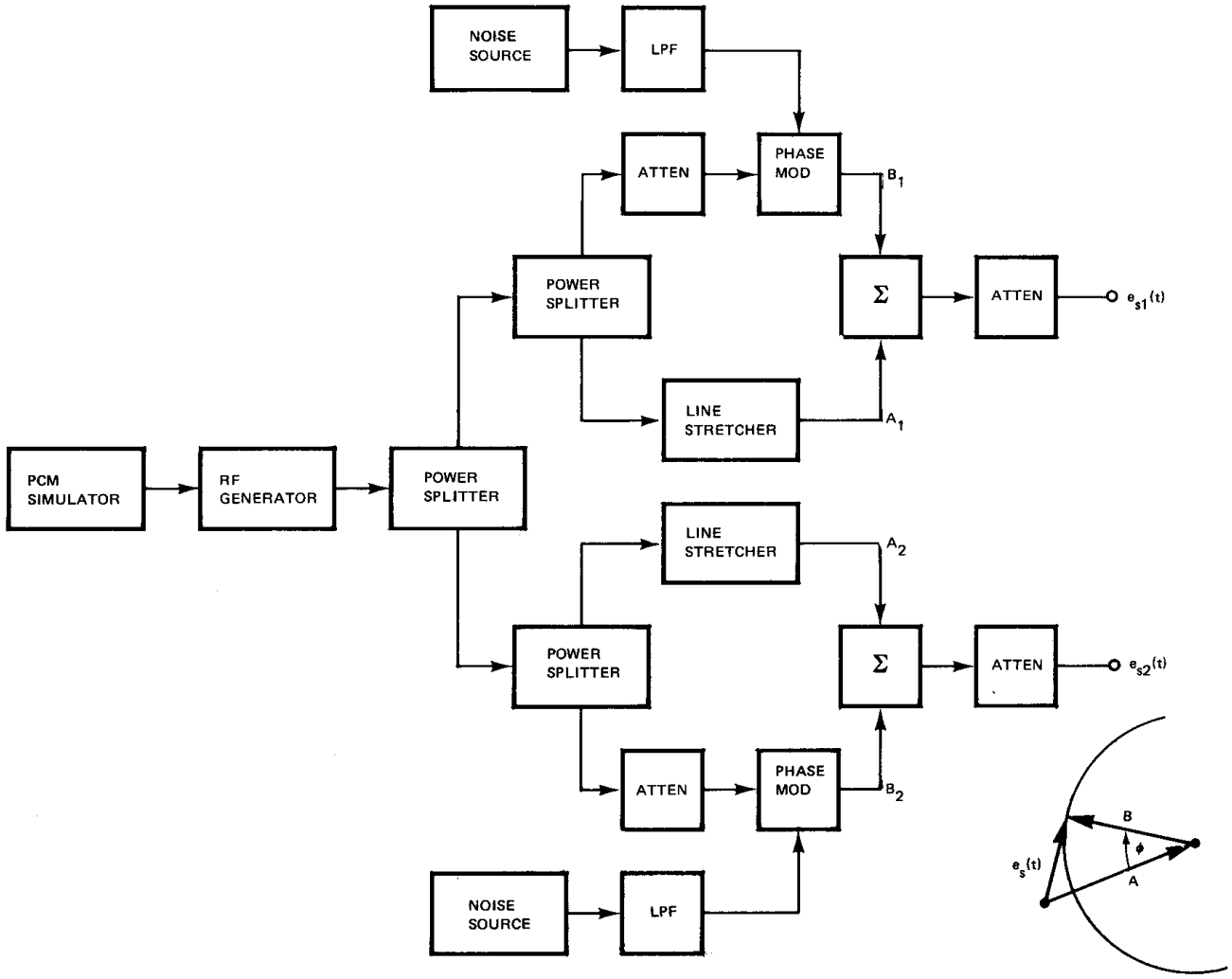

Figure 9. Diversity Signal Simulator Designed to Produce Simultaneous Random Amplitude and Phase Modulation of the Output Signals.

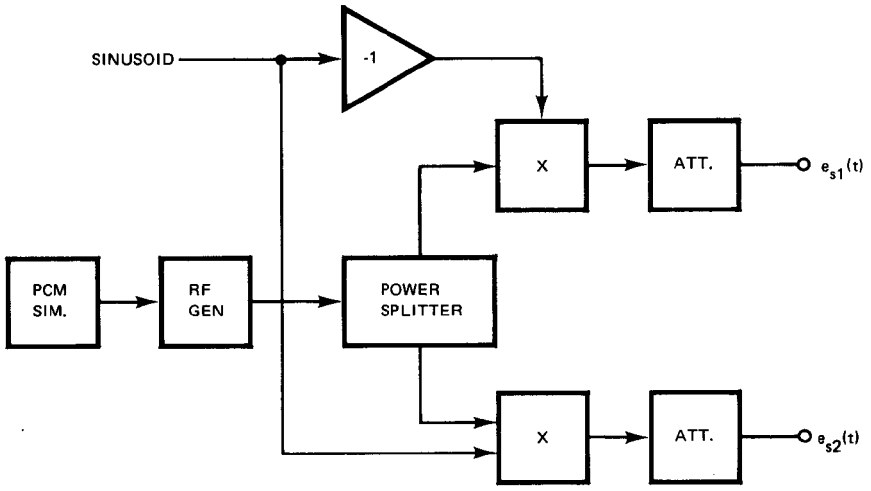

Figure 10. Diagram of Simulator Used to Produce Sinusoidal Out-of-Phase Fading With Minimal Phase modulation.

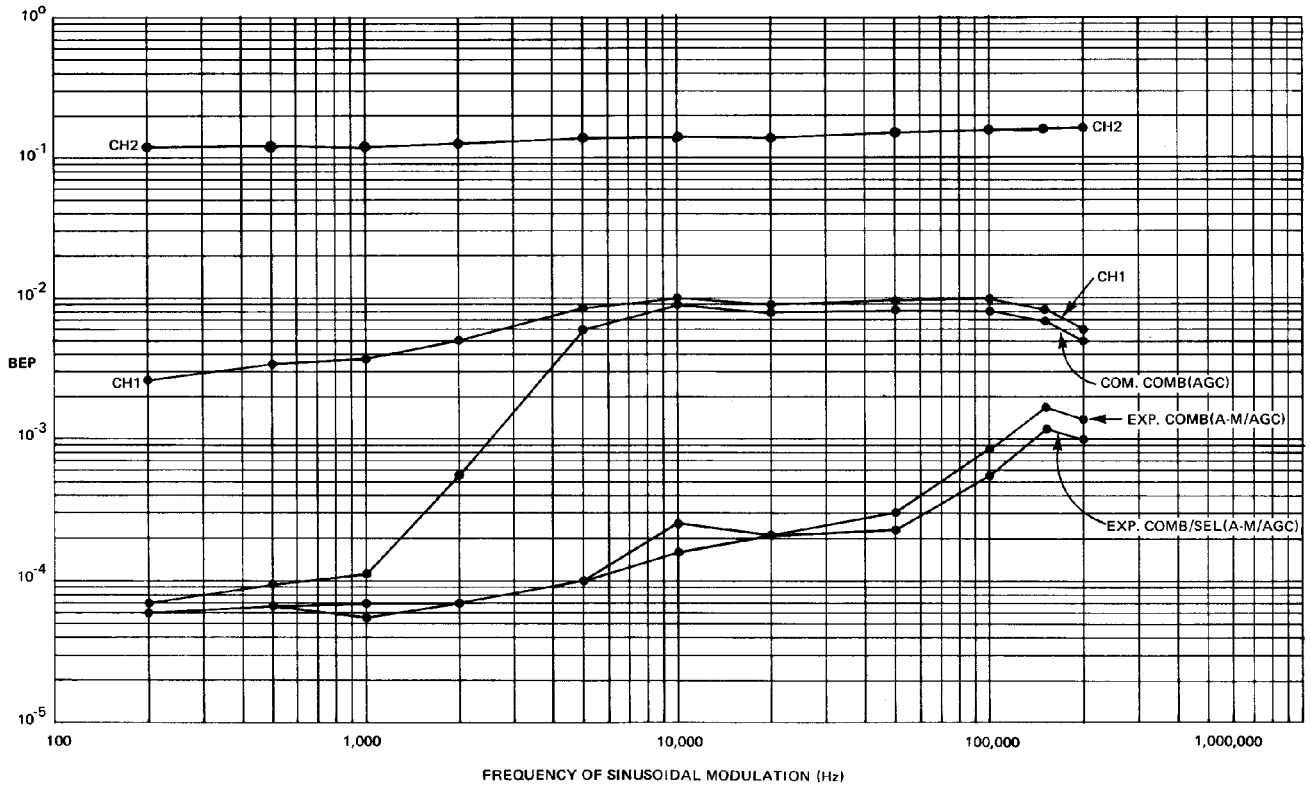

Figure 11. Commercial and Experimatntal Combiner Response to Sinusoidal Out-of-Phase Fading.

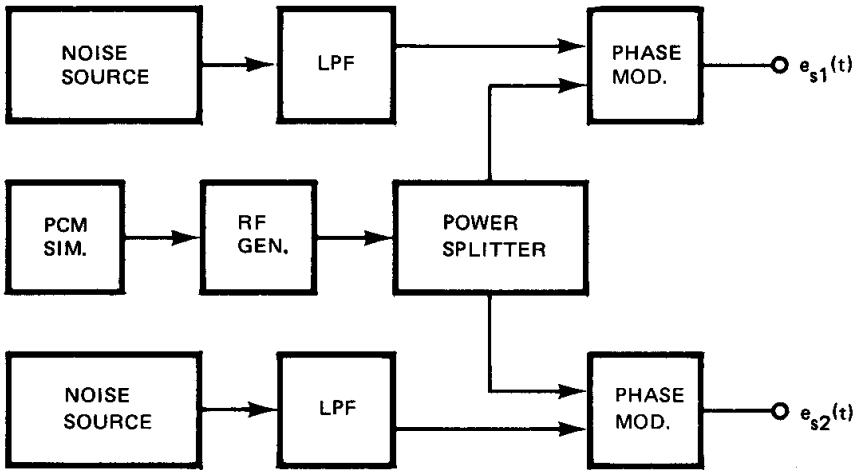

Figure 12. Diagram of Simulator Used to Produce Random Phase Modulation With Minimal Fading.

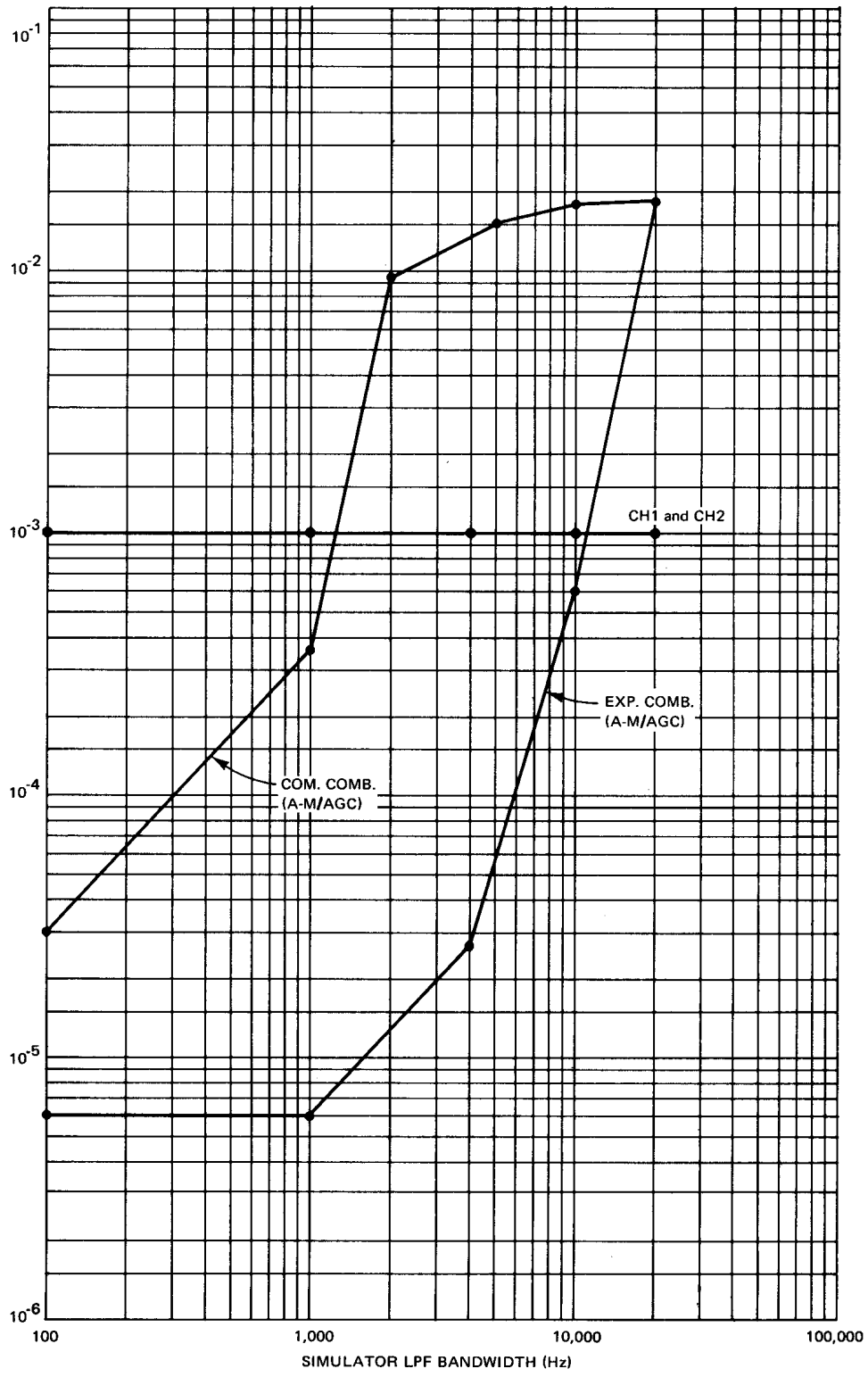

Figure 13. Commercial and Experimetal Combiner Response to Random Phase-Modulated Signals.

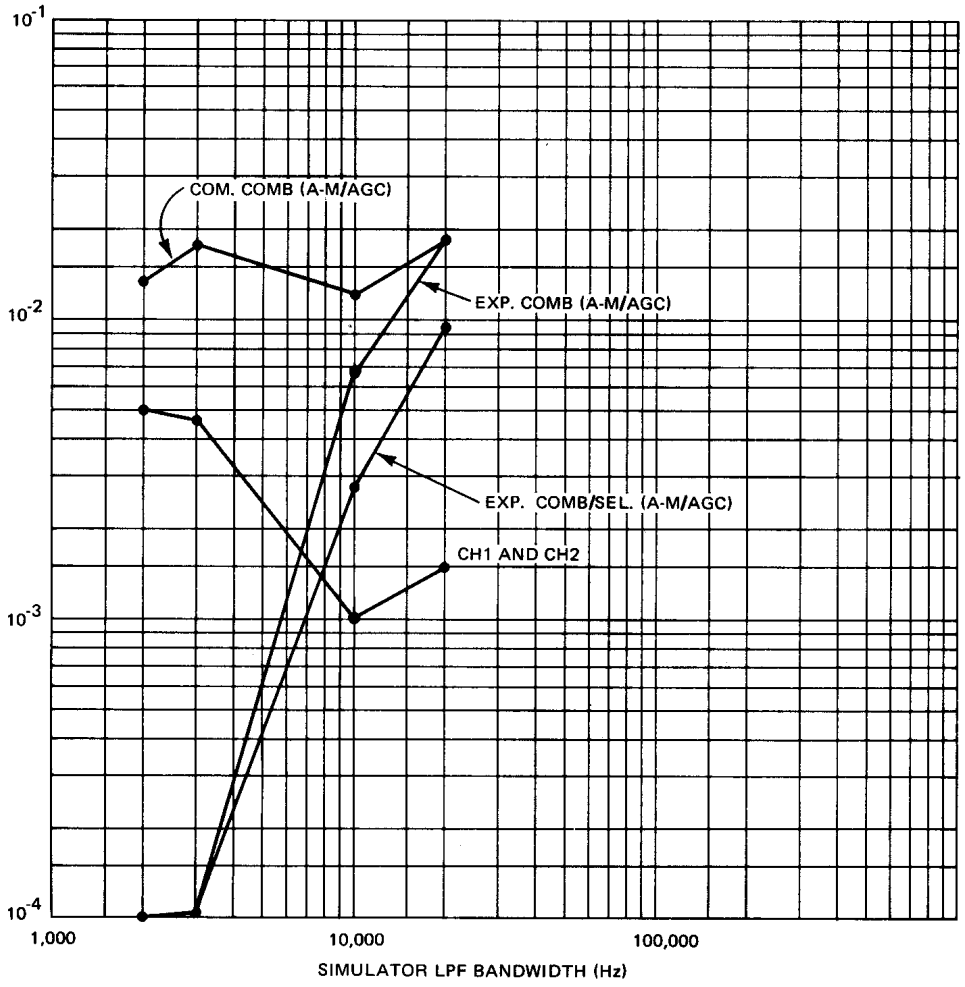

Figure 14. Comparison of Experimental Combiner/Selector With Experimental Combiner With Random Phase-Modulated Signals.

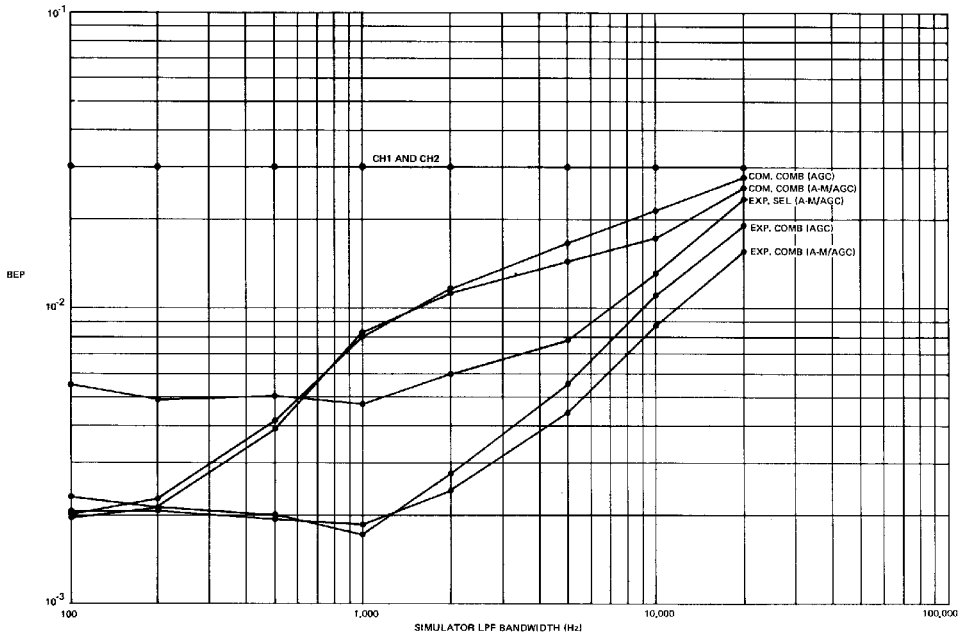

Figure 15. Commercial and Experimental Combiner Response to Signals With Random Amplitude and Phase Modulation.